FERMION LOCALIZATION ON THE DEFORMED BRANE WITH THE DERIVATIVE COUPLING MECHANISM

Masoumeh Moazzen Sorkhi[†], Zahra Ghalenovi

Department of Physics, Faculty of Basic Sciences
Kosar University of Bojnord, Iran

In this paper, by using two localization mechanisms which one is the well-known Yukawa coupling and the other is the new derivative fermion–scalar coupling, we reinvestigate the fermion field localization on deformed branes. These branes are generated by the so-called two-kink solutions, obtained after a deformation of a ϕ^4 potential. The study of deformed defects is important because it contains internal structures which may have implications in braneworld scenarios. Because of existing freedom in the form of the Yukawa coupling, we consider a function of the warp factor for both coupling mechanisms. With two mechanisms, it is shown that massless zero modes of fermion fields are localized on the deformed brane depending on the value of the coupling constant which is independent of the deformation parameter. Moreover, we find that both mechanisms can result in a volcano-like potential of the fermion massive modes associated to the corresponding Schrödinger-like equation. Furthermore, effects of the internal structure on the zero mode and fermion effective potentials are addressed.

1. Introduction

In the last few years, theories involving the braneworld scenario have attracted a lot of interest. The idea of embedding our Universe that might be a *hypersurface* in a higher dimensional space-time suggests many creative ways to solve some problems in new physics, such as cosmological constant problems [1], Casimir force [2] and the gauge hierarchy problem [3]. In the Randall and Sundrum (R–S) model [4], our four-dimensional Universe is generated by a real scalar field which is coupled to gravity minimally.

[†] Corresponding author: `m.m.sorkhi@kub.ac.ir`

Moreover, in this model, the brane is assumed infinitely thin and it does not provide a smallest scale in a fundamental theory. Hence, in more realistic field models, thick branes have been proposed as a smooth generalization of the R–S model where the five-dimensional gravity is coupled to scalar fields minimally [5] and non-minimally [6]. In this scenario, with a specific choice for the scalar potential, the brane is usually generated by a scalar field with kink configuration which provides a domain wall that may be interpreted as non-singular version of the R–S model. A class of topological defect solutions is created starting from a specific deformation of the ϕ^4 potential which may be used to mimic new braneworld containing internal structures [7, 8]. Such internal structures have implications to the way the background space-time is constructed and the way their curvature behaves. Furthermore, the authors of Ref. [6] investigated deformed defects with a non-minimally coupled background scalar field. They found that each *brane* splits into two sub-branes as increasing the non-minimal coupling constant.

In the braneworld theory, the issue of localization of gravity and various bulk matter fields is an interesting subject. This investigation represents us which kind of brane structure is phenomenologically more acceptable. In other studies [9–12], it was shown that the graviton can be localized in the R–S thin brane and thick brane scenarios but it is not true for vector and Kalb–Ramond fields [13, 14]. In order to localize gauge fields, some new mechanisms were introduced in Refs. [15–17]. Besides, it is important to consider the localization problem of the spin-1/2 fermions. Introducing the Yukawa coupling between fermions and background scalar fields, fermions can be localized on branes embedded in a five-dimensional space-time [18, 23]. In Ref. [24], by using the Yukawa coupling term arising from a scalar field ϕ, the issue of fermion localization and resonances was investigated in deformed branes. It was shown that the deformation parameter is very important for localization and normalization of fermionic fields. Moreover, it should be noted that the Yukawa coupling term can be assumed with various forms [25–27]. The authors of Ref. [28] have proposed a more natural Ansatz for the Yukawa coupling in the 5D bulk fermionic action arising from the geometry shape of the warp factor that guarantees the localization of the fermions with right- or left-chirality.

In [29], the authors have considered a new localization mechanism which contained a derivative fermion–scalar coupling term for which the scalar field can be an odd or even function of the extra dimension. If there are even and odd background scalars in the thick brane model, one can also consider both the above-mentioned coupling mechanisms at the same time [30]. In [31], the authors have investigated the localization and spectrum structure of a bulk fermion on the Bloch brane with both the Yukawa coupling and the derivative coupling. Furthermore, in order to localize fermions, the authors of Ref. [32] have introduced a new coupling between a spinor field and

the scalar curvature of space-time. Because of Z_2 symmetry of the extra dimension, their new coupling mechanism can easily deal with the problem encountered in the Yukawa coupling with even background scalar fields. There are many works that study the characteristics of the various matter fields localization in braneworld models. For some comprehensive reviews, see Refs. [33–38].

There are a lot of investigations of fermion fields localization in the setup of the usual Yukawa coupling between fermions and background scalar fields, but for the case of the derivative fermion–scalar coupling, the investigations are limited. In this paper, we are interested to make an analysis of several aspects of localization of the fermion field on deformed branes by using the Yukawa and derivative coupling mechanisms. Presenting the shapes of the mass-independent potentials of KK modes in the corresponding Schrödinger equations, we investigate the localization of massless bulk fermion fields on the deformed brane. More studies on various matter fields localization on deformed branes can be found in Refs. [39–42].

The plan of this paper is as follows. In Section 2, we briefly summarize the deformed braneworld models. In Section 3, we first study the localization of the fermion field on the deformed branes with the Yukawa coupling mechanism. Following the procedure of Ref. [28], we take the Yukawa coupling term as a function of the warp factor. Next, we only consider the derivative fermion–scalar coupling and, finally, we investigate the fermion localization with both coupling mechanisms. In Section 4, the localization condition of the fermion zero mode is discussed for mentioned various couplings. Finally, a summary and conclusion are given in Section 5.

2. The deformed branes

In this section, we consider a thick brane setup constructed by a real scalar field ϕ coupled to gravity minimally. The metric for a brane which is embedded in a five-dimensional AdS space is given by

$$\mathrm{d}s^2 = g_{MN}\mathrm{d}x^M\mathrm{d}x^N = e^{2A(y)}g_{\mu\nu}\mathrm{d}x^\mu\mathrm{d}x^\nu + \mathrm{d}y^2 \,. \tag{1}$$

The warp factor is expressed in terms of the function $A(y)$, where y is the extra dimension and the $g_{\mu\nu} = (-1, +1, +1, +1)$ is the Minkowski metric. In order to construct the deformed brane solution, we start with the following action for a bulk scalar field coupled to gravity as [39]:

$$S = \int \mathrm{d}^5x\sqrt{-g}\left[\frac{1}{2\kappa_5^2}R - \frac{1}{2}g^{MN}\partial_M\phi\partial_N\phi - V(\phi)\right] \,, \tag{2}$$

where R is the five-dimensional scalar curvature. The $\kappa_5^2 = 4\pi G_5$, where the G_5 is the five-dimensional Newton constant. We also notice that such

a scalar field ϕ depends only on the extra dimension y. The equations of motion resulting from action (2) are

$$3\left(A'' + 2A'^2\right) + \frac{1}{2}\phi'^2 + V(\phi) = 0, \tag{3}$$

$$6A'^2 - \frac{1}{2}\phi'^2 + V(\phi) = 0, \tag{4}$$

$$-\phi'' - 4A'\phi' + \frac{\mathrm{d}V(\phi)}{\mathrm{d}\phi} = 0, \tag{5}$$

where we have set $\kappa_5^2 = 1$. We also note that the prime means derivative with respect to y. We now apply the first order formalism to the braneworld scenario initially introduced in Ref. [43]. The method consists of a function $W(\phi)$ called superpotential function in such a way that

$$A' = -\frac{1}{3}W(\phi) \tag{6}$$

and

$$\frac{\partial W(\phi)}{\partial \phi} = \phi'. \tag{7}$$

The solutions of Eqs. (6) and (7) are the solutions of the equations of motion (3)–(5). It should be mentioned that in the equations of motion, the potential $V(\phi)$ is written as a function of a superpotential $W(\phi)$. As was considered in Refs. [39–42], we define the potential $V(\phi)$ in the form of

$$V(\phi) = \frac{1}{2}\left(\frac{\partial W}{\partial \phi}\right)^2 - \frac{2}{3}W^2. \tag{8}$$

Following Refs. [39–42], the superpotential is given by

$$W(\phi) = \frac{p}{2p-1}\phi^{\frac{2p-1}{p}} - \frac{p}{2p+1}\phi^{\frac{2p+1}{p}}, \tag{9}$$

where p is an odd integer. The form for $W(\phi)$ can be obtained by deforming the usual ϕ^4 model and it is introduced in the study of deformed branes [44]. From the choice of the superpotential $W(\phi)$ and using potential (8), the equations of motion can be easily solved, and the function $A(y)$ and the background scalar $\phi(y)$ can be obtained as

$$A(y) = -\frac{1}{6}\frac{p}{2p+1}\tanh^{2p}\left(\frac{y}{p}\right) - \frac{1}{3}\left(\frac{p^2}{2p-1} - \frac{p^2}{2p+1}\right)$$

$$\times \left\{ \ln\left(\cosh\left(\frac{y}{p}\right)\right) - \sum_{i=1}^{p-1}\frac{1}{2i}\tanh^{2i}\left(\frac{y}{p}\right) \right\}, \tag{10}$$

$$\phi(y) = \tanh^p\left(\frac{y}{p}\right). \tag{11}$$

We note that the exponential warp factor constructed with the function $A(y)$ is localized at the center of the brane, $y = 0$, and for the large y, its behavior is similar to the R–S braneworld model. What is more, the warp factor affects the characteristics of fields localization and the construction of effective actions in $D = 4$. Furthermore, equation (11) gives us the solutions of the scalar field that are the usual kink solution for $p = 1$ and deformed solutions with a two-kink profile for odd $p > 1$. Such deformations suggest the existence of an internal structure which has implications in the density of matter-energy along the extra dimension [44]. In the braneworld theory, the continuous deformation from a single brane to two sub-branes, by varying parameters, is called the phenomenon of brane splitting [44–46].

3. Localization of fermions

In this section, we study the localization of bulk fermion field in deformed braneworld model generated by a scalar field. When the background scalar field is an odd function of the extra dimension, the well-known Yukawa coupling between fermions and the scalar field is used in order to get a localized mode. The non-Yukawa derivative coupling mechanism is employed in order to solve the problem of fermion localization on an even background scalar field. In [24], localization of fermions on deformed brane with the usual Yukawa coupling was investigated. In this work, we are interested to know what happens when one tries to introduce a non-Yukawa coupling term in the bulk fermion field action. We discuss the localization of the bulk fermion fields by analyzing the analog quantum mechanical potential of the corresponding Schröödinger equation for their KK modes. Let us consider the action of a massive bulk fermion field which is coupled to gravity as [31]

$$S = \int \mathrm{d}^5 x \sqrt{-g} \left(\bar{\Psi}\Psi^M(\partial_M + \omega_M)\Psi - \eta\bar{\Psi}F_1(y)\Psi + \lambda\bar{\Psi}\Psi^M\partial_M F_2(y)\gamma^5\Psi \right), \tag{12}$$

where η and λ are the coupling constants between fermions and scalar and ω_M is the spin connection. $F_1(y)$ and $F_2(y)$ are some general scalar functions of the extra dimensional coordinate y. We will discuss properties of the

scalar functions later. The metric is given by equation (1), but it is more convenient to change it to a conformal flat metric as

$$ds^2 = e^{2A(z)} \left(g_{\mu\nu} dx^\mu dx^\nu + dz^2 \right) . \tag{13}$$

From action (12) and metric (13), the equation of motion for the fermion field can be expressed as

$$\frac{1}{\sqrt{-g}} \left[\gamma^\mu \partial_\mu + \gamma^5 \left(\partial_z + 2\dot{A} \right) - \eta e^A F_1(y(z)) + \lambda \dot{F}_2(y(z)) \right] \Psi = 0 , \tag{14}$$

where the relation of the new coordinate z and y is $dz = e^{-A(y)} dy$, and the dot denotes the derivative with respect to the extra dimension z. In order to solve the above equation, we use the following chiral decomposition:

$$\Psi(x,y) = e^{-2A} \sum_n (\psi_{Ln}(x) f_{Ln}(z) + \psi_{Rn}(x) f_{Rn}(z)) , \tag{15}$$

with $\psi_{Ln}(x) = -\gamma^5 \psi_{Ln}(x)$ and $\psi_{Rn}(x) = \gamma^5 \psi_{Rn}(x)$. With this decomposition, $\psi_{Ln}(x)$ and $\psi_{Rn}(x)$ are the left-handed and right-handed components of the four-dimensional *spinor* field, respectively, which satisfy the following four-dimensional Dirac equations:

$$\gamma^\mu \partial_\mu \psi_{Ln}(x) = m_n \psi_{Rn}(x) , \tag{16}$$
$$\gamma^\mu \partial_\mu \psi_{Rn}(x) = m_n \psi_{Ln}(x) . \tag{17}$$

Moreover, the fermion KK modes, the $f_{Rn}(z)$ and $f_{Ln}(z)$, satisfy

$$\left[\partial_z + \eta e^A F_1 - \lambda \partial_z F_2 \right] f_{Ln}(z) = m_n f_{Rn}(z) , \tag{18}$$
$$\left[\partial_z - \eta e^A F_1 + \lambda \partial_z F_2 \right] f_{Rn}(z) = -m_n f_{Ln}(z) . \tag{19}$$

The above equations can be given as the following Schrödinger-like equations:

$$[-\partial_z^2 + V_L(z)] f_{Ln}(z) = m_n^2 f_{Ln}(z) , \tag{20}$$
$$[-\partial_z^2 + V_R(z)] f_{Rn}(z) = m_n^2 f_{Rn}(z) . \tag{21}$$

The differential equations (20) and (21) give us information about the zero and massive modes of the bulk fermion field. The effective potentials $V_L(z)$ and $V_R(z)$ are

$$V_L(z) = \left(\eta e^A F_1 \right)^2 - \eta e^A \left(\dot{A} F_1 + \dot{F}_1 \right) - 2\eta\lambda e^A F_1 \dot{F}_2 + \lambda^2 \dot{F}_2^2 + \lambda \ddot{F}_2 , \tag{22}$$
$$V_R(z) = V_L(z) \big|_{\lambda \to -\lambda,\, \eta \to -\eta} . \tag{23}$$

However, it is difficult to obtain an analytical expression for the function $A(z)$. This means that the potential $V_{\mathrm{L,R}}(z)$ must be studied numerically. For this purpose, we write the expression of $V_{\mathrm{L,R}}(z)$ in the y coordinate by the use of the coordinate transformation $\mathrm{d}z = e^{-A(y)}\mathrm{d}y$, and the results are

$$
\begin{aligned}
V_{\mathrm{L}}(z(y)) &= \left(\eta e^{A} F_1\right)^2 - \eta e^{2A}\left(A' F_1 + F_1'\right) - 2\eta\lambda e^{2A} F_1 F_2' \\
&\quad + \lambda e^{2A}\left(\lambda F_2'^2 + A' F_2' + F_2''\right),
\end{aligned} \tag{24}
$$

$$
V_{\mathrm{R}}(z(y)) = V_{\mathrm{L}}(z(y))\big|_{\lambda \to -\lambda,\,\eta \to -\eta}. \tag{25}
$$

In order to derive the effective action on the brane for the four-dimensional massless and massive Dirac fermions, we need the following orthonormality conditions for the KK modes $f_{\mathrm{R}n}(z)$ and $f_{\mathrm{L}n}(z)$ [29]:

$$
\int_{-\infty}^{+\infty} f_{\mathrm{L}m} f_{\mathrm{L}n}\mathrm{d}z = \int_{-\infty}^{+\infty} f_{\mathrm{R}m} f_{\mathrm{R}n}\mathrm{d}z = \delta_{mn}, \tag{26}
$$

$$
\int_{-\infty}^{+\infty} f_{\mathrm{L}m} f_{\mathrm{R}n}\mathrm{d}z = 0. \tag{27}
$$

Potentials (24) and (25) depend on the warp factor exponent $A(y)$ and the functions $F_1(y)$ and $F_2(y)$. It should be mentioned that in order to get an effective potential with Z_2 symmetry along the extra dimension, $F_1(y)$ and $F_2(y)$ should be odd and even functions of y respectively. The two coupling functions F_1 and F_2 can be taken as various forms of background scalar field and warp factor. In [31], these functions are made of a background scalar field ϕ, while in Refs. [28, 29], they were considered to be functions of the warped factor $A(y)$ and its derivative. In [28], the authors have found a way to choose the function F_1 as a function of derivatives of the warp factor by directly looking at the integrability conditions on the left- and right-handed fermion zero mode in Schrödinger-like equations (18) and (19). Furthermore, in order to localize fermions on a two-field-thick brane, the authors of Ref. [29] have considered $F_2 = A(y)$ as the non-Yukawa derivative coupling between fermions and the background scalar field. Moreover, we mention that these sorts of couplings have been used for localization of other matter fields such as vector and tensor gauge fields [36, 47]. For example, in [47], Stueckelberg-like Kalb–Ramond and gauge fields localization have been explored on a thick brane through a suitable modification of the Yukawa coupling which is described by a function of derivatives of the warp factor. In this work, following the procedure of Refs. [28] and [29], and considering that solutions for the background scalar field (11) and warp factor (10) are,

respectively, odd and even function of extra dimension, we assume the simple choices $F_1(y) = \partial_y^n A(y)$ and $F_2(y) = A^m(y)$, where m and n are positive integer numbers. Note that the coupling functions F_1 and F_2 in Refs. [28] and [29] are only one case of our work with $m = 1$, $n = 1$.

By considering the behavior of the effective potentials (24) and (25), we can study the localization of the fermion field on the deformed brane. In order to get a localized zero mode, the value of the effective potential at its minimum must be negative. What is more, the asymptotical behavior of the potentials gives us information about the presence of gaps in the continuum spectrum of KK massive modes. The massive KK modes can be solved numerically, but we do not discuss them in this paper. In the following discussion, we will first investigate the effective potentials for the case of the Yukawa coupling with $\eta \neq 0$ and $\lambda = 0$, then we consider other couplings containing derivative coupling terms with $\lambda \neq 0$.

3.1. The Yukawa coupling

It is well-known that the Yukawa coupling between the scalar and *spinor* is a necessary condition for fermions to be localized on a brane. In [24], it was shown that by using $F_1(y) = \phi$, where the ϕ is the background scalar field, the fermion can be localized on deformed branes. In this subsection, we propose a new form for the Yukawa coupling that includes a function of the warp factor and investigates the fermion localization. Here, we will focus on the fermion localization on the deformed brane with the Yukawa coupling mechanisms by setting $\eta \neq 0$ and $\lambda = 0$. Under this considerations, Eqs. (24) and (25) are rewritten as

$$V_L(z(y)) = \left(\eta e^A F_1\right)^2 - \eta e^{2A}\left(A'F_1 + F'_1\right), \tag{28}$$

$$V_R(z(y)) = V_L(z(y))\big|_{\eta \to -\eta}. \tag{29}$$

We set the Yukawa coupling term as a function of the warp factor $A(y)$ such that

$$F_1(y) = \partial_y^n A(y). \tag{30}$$

Regarding the solution of the warp factor in equation (10), we find that the n should be an odd number to ensure the effective potentials $V_{L,R}(z(y))$ to be even function of the extra dimension. By setting Eq. (30) into Eq. (28), we have

$$V_L(z(y)) = \eta^2 e^{2A}\left(\partial_y^n A\right)^2 - \eta e^{2A}\left(A'\partial_y^n A + \partial_y^{n+1} A\right) \tag{31}$$

and

$$V_R(z(y)) = V_L(z(y))\big|_{\eta \to -\eta}. \tag{32}$$

For simplicity, we assume that $n = 1$, thus we get

$$V_{\mathrm{L}}(z(y)) = \eta e^{2A} \left[(\eta - 1)A'^2 + A'' \right] , \qquad V_{\mathrm{R}}(z(y)) = V_{\mathrm{L}}(z(y)) \big|_{\eta \to -\eta} . \quad (33)$$

The values of the effective potentials at $y = 0$ are

$$V_{\mathrm{L}}(0) = -V_{\mathrm{R}}(0) = \left\{ \begin{array}{ll} \frac{\eta}{3} & p = 1 , \\ 0 & p \geq 3 , \end{array} \right. \quad (34)$$

in which we have used the following initial conditions for the warp factor A:

$$A(0) = A'(0) = 0 . \quad (35)$$

Considering the asymptotic behaviors of the background scalar field which are $\phi(y) \to \pm 1$, $\phi' \to 0$ and $\phi'' \to 0$, we can also find the asymptotic behavior of the warp factor at $y \to \pm\infty$. From Eqs. (3) and (4), the asymptotical form of the warp factor can be given as $e^{A(y)} \to e^{-\frac{|y|}{p}}$, which is similar to the R–S braneworld model. By considering the asymptotic behavior of the warp factor and the background scalar, the asymptotic behavior of the potentials $V_{\mathrm{L}}(y)$ and $V_{\mathrm{R}}(y)$ as $y = \pm\infty$ is

$$V_{\mathrm{L,R}}(y \to \pm\infty) = 0 \qquad \text{for all values of } p \text{ and } n . \quad (36)$$

The effective potentials (31) and (32) are plotted for various values of n and p in Figs. 1–3. In Figs. 1 and 2, the effect of the n on the effective potential is shown for $p = 1$ and $p = 3$ respectively. We also consider the effect of the deformation parameter p on the effective potential in Fig. 3. From Eq. (34) as well as Fig. 1 (left), we find that for the cases of $n = 1$ and
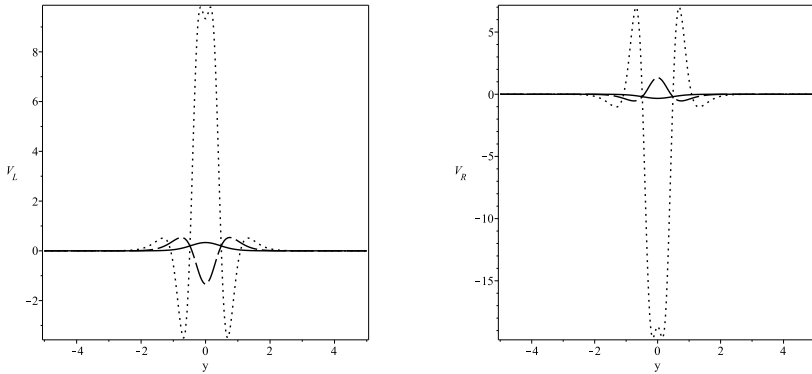

Fig. 1. The profile of the potentials (left) $V_{\mathrm{L}}(y)$ and (right) $V_{\mathrm{R}}(y)$ for $n = 1$ (solid line), $n = 3$ (dashed line), $n = 5$ (dotted line), $\lambda = 0$, $p = 1$, $\eta = 1$.

$p = 1$, the left-handed potential has a positive value at the brane location when $\eta > 0$ which means that the left-handed massless fermion cannot be localized on the brane, while right-handed potential has a negative value at its minimum and the zero mode of the right-handed fermion can be trapped. As it is seen in Fig. 1, for $n \geq 3$, both cases of the effective potentials have one (or two minima) with a negative value which means that the left- and right-handed fermion may be localized on the deformed brane.

In Figs. 2 (left) and 2 (right), the effect of the parameter n on the effective potentials V_L and V_R with $p = 3$ is shown. From these figures, we find that the effective potentials have an inner structure with different values of n. Furthermore, it is seen that the height as well as the depth of the potential increase with n. As Figs. 1 and 2 show, the effective potentials $V_{L,R}(y)$ tend to vanish at the infinity of the extra dimension, $V_{L,R}(y \to \pm\infty) \to 0$, and the shape of these potentials looks like a volcano which means that the mass spectrum of the fermion field is continued. We also study the effect of the
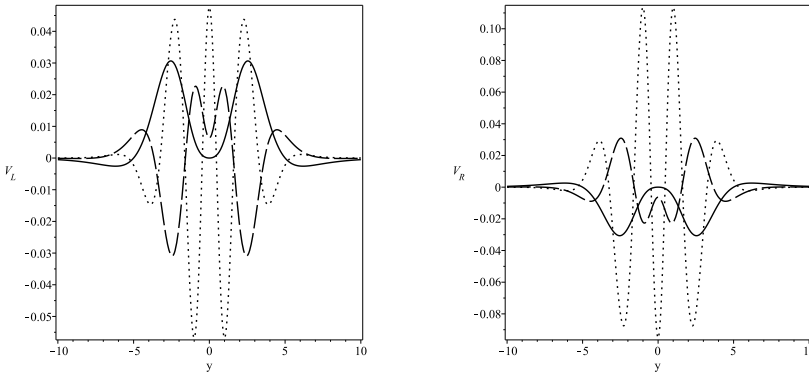

Fig. 2. The profile of the potentials (left) $V_L(y)$ and (right) $V_R(y)$ for $n = 1$ (solid line), $n = 3$ (dashed line), $n = 5$ (dotted line), $\lambda = 0$, $p = 3$, $\eta = 1$.

deformation parameter p on the effective potential V_L in Fig. 3 for $n = 1$ and $\eta = -1$. In this figure, we see that the effective potential $V_L(y)$ has a deep minimum only for $p = 1$ but the minimum splits into two minima when $p \geq 3$ which indicates that increasing the parameter p can make the brane splitting from a single-brane to two sub-branes for the single-kink background scalar field. Moreover, the distance between the two minima of $V_L(y)$ increases when the parameter p increases. Furthermore, we can find that when the p becomes larger, the values of the two maxima of the potential, as well as the depth of the wells, decrease. This is an important feature since the resonant modes occurs for $m_n^2 \leq V_{\max}$. The study of the resonances is important since it can give relevant information on the coupling of massive modes and the brane, illustrating how the mechanism of
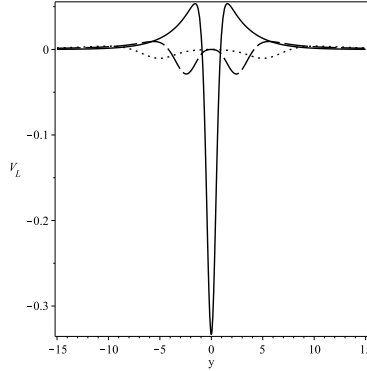
Fig. 3. The profile of the potential $V_{\mathrm{L}}(y)$ for $p = 1$ (solid line), $p = 3$ (dashed line), $p = 5$ (dotted line), $\eta = -1$, $n = 1$, $\lambda = 0$.

the field trapping is being processed. Using a well-known resonance detecting method [25, 48], one can analyze the resonant modes arising from equations (20) and (21). The authors of Ref. [49] used the Numerov method [50, 51] and the Runge–Kutta fourth-order method to investigate massive modes and their contribution to gravity localization on thick branes. They found that the Numerov method can be used when the effective potential is only known numerically, while the Runge–Kutta method appears to be inadequate when the potential is not known analytically. Furthermore, in Refs. [25, 31], the relative probability [48] and transmission coefficient methods [52–54] were used to find fermion KK resonances.

3.2. The derivative coupling

Now, we study the fermion localization with the derivative coupling mechanism by setting $\eta = 0$. Under this assumption, the effective potentials $V_{\mathrm{L,R}}$ in equations (24) and (25) can be rewritten as

$$V_{\mathrm{L}}(z(y)) = \lambda e^{2A} \left[\lambda F'^2_2 + \lambda F'_2 + F''_2 \right], \qquad V_{\mathrm{R}}(z(y)) = V_{\mathrm{L}}(z(y))\big|_{\lambda \to -\lambda}. \tag{37}$$

We now consider the following form for the function $F_2(y)$:

$$F_2(y) = A^m(y). \tag{38}$$

We note that for all odd and even values of m, the function $F_2(y)$ is an even function of the extra dimension y so the effective potential preserve its Z_2 symmetry. By substituting Eq. (38) into Eq. (37), we get

$$V_{\mathrm{L}}(y) = \lambda e^{2A}$$
$$\times \left[\lambda m^2 A'^2 A^{2(m-1)} + m A'^2 A^{(m-1)} + m A'' A^{(m-1)} + m(m-1) A'^2 A^{(m-2)} \right]. \tag{39}$$

By considering the initial conditions of the warp factor and the background scalar field at $y = 0$, the values of the potentials at the origin can be obtained as

$$V_{\text{L}}(0) = -V_{\text{R}}(0) = \begin{cases} -\frac{\lambda}{3} & p = 1, \quad m = 1, \\ 0 & \text{for other values of } p \text{ and } m. \end{cases} \tag{40}$$

Next, by using the asymptotic behavior of the warp factor and the background scalar field, the asymptotic behavior of the potential at infinity is

$$V_{\text{L,R}}(y \to \pm\infty) = 0 \qquad \text{for all values of } p \text{ and } m, \tag{41}$$

which is similar to a volcano-type potential. The shapes of the effective potentials for the left- and right-handed fermions with different values of m are shown in Figs. 4 and 5 for a positive value of λ. As Fig. 4 shows,
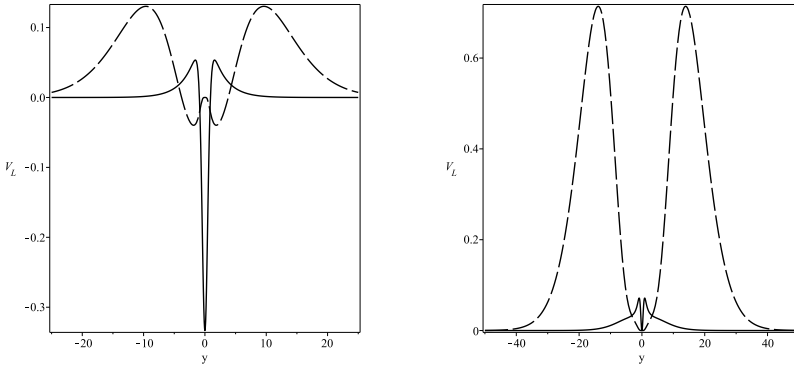

Fig. 4. The profile of the potential $V_{\text{L}}(y)$ for (left) $m = 1$ (solid line), $m = 3$ (dashed line), (right) $m = 2$ (solid line), $m = 4$ (dashed line). The parameters are set to $\lambda = 1$, $p = 1$, $\eta = 0$.

when the m is an odd number, the value of the effective potential V_{L} at its minimum (or minima) is negative which means the left-handed fermion may be localized on the brane, while for even numbers of m, the minimum of the V_{L} is not negative, therefore, the potential does not support a zero-mode. From Fig. 5, we find that the right-handed fermion can be trapped when the value of m is even. In addition, it is seen that the height of the potentials as well as the distance between two maxima increases with increasing the parameter m.

Furthermore, we consider the effect of the deformation parameter p on the left-handed effective potential in Fig. 6 for both cases of the even and odd values of m. As it is seen, similar to the previous subsection, by increasing the p, the height of the potential as well as the distance between two maxima decreases. We also find that the splitting of the minimum does not occur due to increasing the parameter p when the m is an even number.
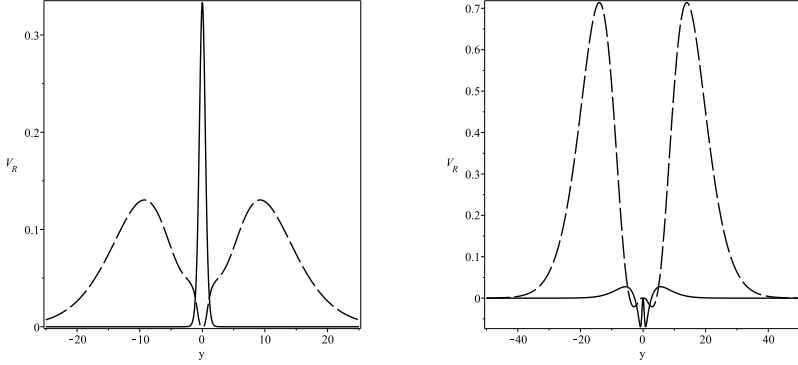
Fig. 5. The profile of the potential $V_{\mathrm{R}}(y)$ for (left) $m = 1$ (solid line), $m = 3$ (dashed line), (right) $m = 2$ (solid line), $m = 4$ (dashed line). The parameters are set to $\lambda = 1$, $p = 1$, $\eta = 0$.
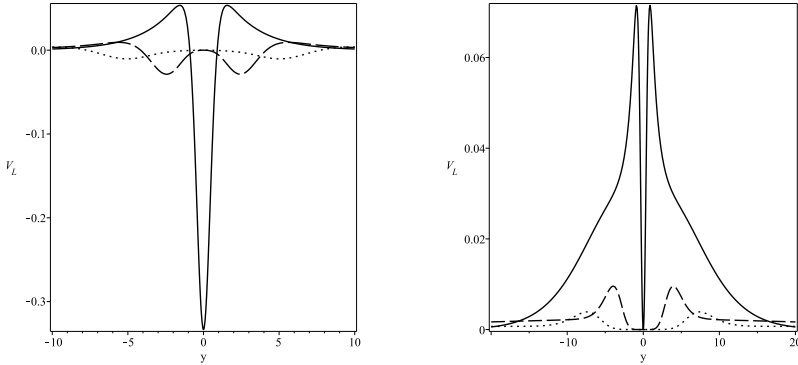

Fig. 6. The profile of the potential $V_{\mathrm{L}}(y)$ for (left) $m = 1$, (right) $m = 2$. The parameters are set to $\lambda = 1$, $\eta = 0$ and $p = 1$ (solid line), $p = 3$ (dashed line), $p = 5$ (dotted line).

3.3. The Yukawa and derivative couplings

Now, we would like to know what will happen to the fermion localization mechanism if we consider both the Yukawa coupling and the derivative coupling. Here, we take into account both the Yukawa and derivative couplings with $\eta \neq 0$ and $\lambda \neq 0$ for the localization of a bulk fermion on deformed branes. The effective potentials $V_{\mathrm{L,R}}(y)$ with the two couplings can be obtained directly according to Eqs. (24) and (25), but we do not present them here. In the following, we will investigate the behavior of the effective potential with $F_1(y) = \partial^n A(y)$ and $F_2(y) = A^m(y)$. For simplicity, we will focus on the cases of $m = 1$ and $n = 1$ which result in the following forms for the effective potentials:

$$V_{\mathrm{L}}(z(y)) = \gamma e^{2A}\left[(\gamma - 1)A'^{2} + A'\right], \qquad V_{\mathrm{R}}(z(y)) = V_{\mathrm{L}}(z(y))\big|_{\gamma \to -\gamma}, \quad (42)$$

where

$$\gamma = \lambda - \eta. \tag{43}$$

The values of the effective potentials at $y = 0$ and $y \to \pm\infty$ can be easily found as

$$V_{\mathrm{L}}(0) = -V_{\mathrm{R}}(0) = \left\{ \begin{array}{cc} -\frac{\gamma}{3} & p = 1, \\ 0 & p \geq 3, \end{array} \right. \tag{44}$$

$$V_{\mathrm{L,R}}(y \to \pm\infty) = 0 \qquad \text{for all values of } p. \tag{45}$$

In Fig. 7, the profile of the left-handed effective potential is shown for two cases of $\gamma > 0$ and $\gamma < 0$. From the figure, we find that for the $p = 1$, the effective potential $V_{\mathrm{L}}(y)$ has a negative value at $y = 0$ when $\gamma > 0$, so that the left-handed zero mode may be localized on the brane, while for
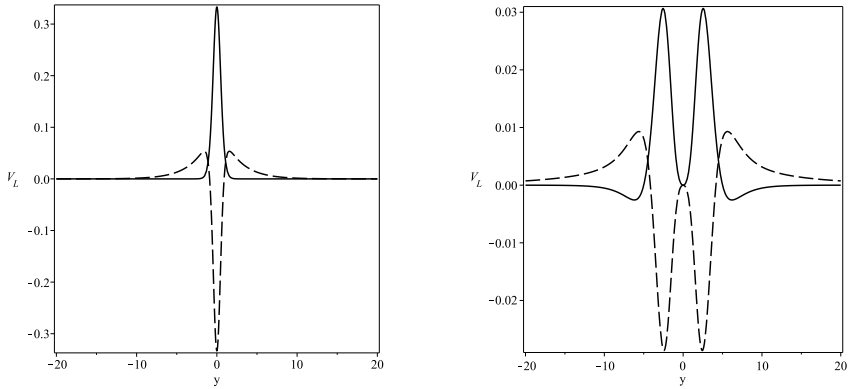

Fig. 7. The profile of the potential $V_{\mathrm{L}}(y)$ for (left) $p = 1$, (right) $p = 3$. The parameters are set to $n = 1$, $m = 1$ and $\gamma = -1$ (solid line), $\gamma = 1$ (dashed line).

other values of p, the massless mode may be trapped for both signs of γ. By numerical investigation, we also find that increasing the value of the constant γ, the maxima as well as the minima of the potential are raised. Furthermore, shapes of effective potentials (24) and (25) are plotted in Fig. 8 for the case of $p = 1$ with different values of n and m.
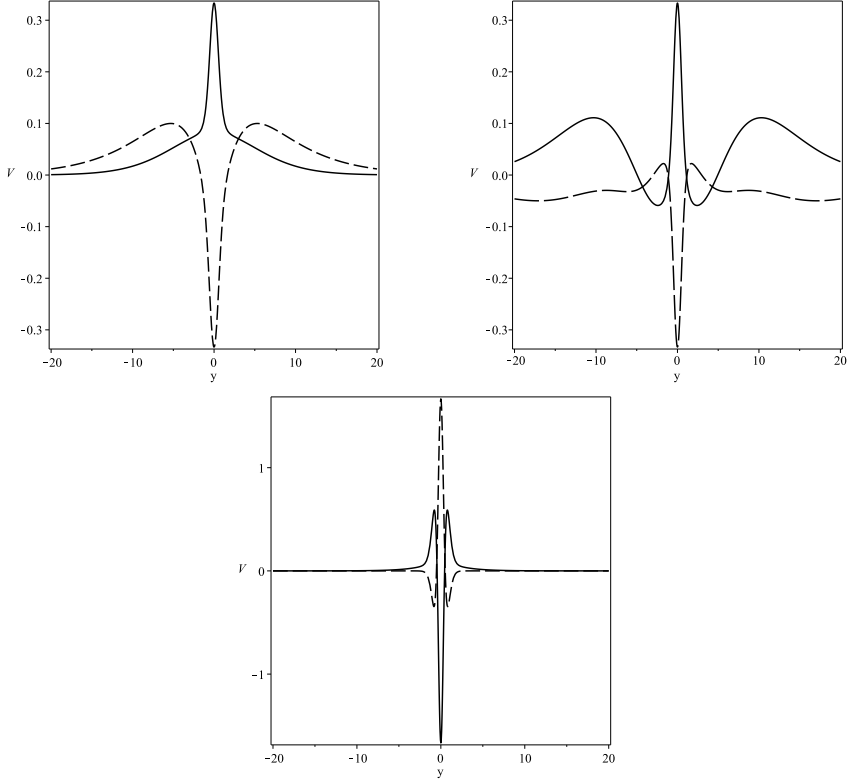
Fig. 8. The profile of the potentials $V_{\mathrm{L}}(y)$ (solid line) and $V_{\mathrm{R}}(y)$ (dashed line) for (top left) $n = 1$, $m = 2$ (top right) $n = 1$, $m = 3$ (bottom) $n = 3$, $m = 1$. The parameters are set to $p = 1$, $\eta = 1$ and $\lambda = 1$.

4. The localized zero mode

In this section, we focus on the calculation of the zero mode under three localization mechanisms discussed in the previous section. By setting $m_n = 0$ in Eqs. (20) and (21), we get the solution of the fermion zero modes as

$$f_{\mathrm{L}0}(y) \propto \exp\left[\lambda F_2(y) - \eta \int_0^z e^{A(z')} F_1(y) \mathrm{d}z'\right]$$

$$= \exp\left[\lambda F_2(y) - \eta \int_0^y F_1\left(y'\right) \mathrm{d}y'\right], \tag{46}$$

$$f_{\mathrm{R}0}(y) = f_{\mathrm{L}0}(y)\big|_{\eta \to -\eta,\, \lambda \to -\lambda}. \tag{47}$$

In order to localize the zero mode, the normalization conditions (26) and (27) must be satisfied. With the relation between y and z which is $dz = e^{-A}dy$, the normalization condition of the left-handed fermion zero mode is rewritten as

$$\int_{-\infty}^{\infty} dy \exp\left[2\lambda F_2(y) - A(y) - 2\eta \int_0^y F_1\left(y'\right) dy'\right] < \infty. \qquad (48)$$

This result shows that the behaviors of the functions $F_1(y)$ and $F_2(y)$ play a leading role for fermion localization on the deformed brane. It should be mentioned that due to the complicated form of the warp factor, it is difficult to investigate Eq. (48) analytically. However, following the same procedure of Refs. [6, 23], we only need to consider the asymptotic behavior of the integrand. From now on, we discuss the normalization condition (48) and the zero mode solution (46) for various coupling mechanisms considered in Section 3.

For the case of Yukawa coupling mechanism, by setting $\lambda = 0$ and using $F_1 = \partial_y^n A(y)$, where n is an odd number, the normalization condition (48) is equivalent to the following conditions for all values of p:

$$\int_{-\infty}^{\infty} dy \exp[-(1 + 2\eta)A(y)], \qquad n = 1, \qquad (49)$$

$$\int_{-\infty}^{\infty} dy \exp\left[-A(y) - 2\eta\partial_y^{n-1}A(y)\right], \qquad n \geq 3. \qquad (50)$$

Considering the asymptotic behavior of the warp factor, $A(\pm\infty) = -\frac{|y|}{p}$, the asymptotic behavior of integrand in Eqs. (50) and (49), named as I_0, at $y \to \infty$, is

$$I_0 = \begin{cases} \exp\left((1 + 2\eta)\frac{|y|}{p}\right), & n = 1, \\ \exp\left(\frac{|y|}{p}\right), & n \geq 3. \end{cases} \qquad (51)$$

It can be easily found that the normalization condition for the left-handed fermion zero mode for the Yukawa coupling mechanism is

$$n = 1 \quad \text{and} \quad \eta < -\frac{1}{2}. \qquad (52)$$

Therefore, under condition (52), the left-handed zero mode is localized on the deformed brane with the Yukawa coupling mechanism. Note that the normalization condition for this case is independent of p, while in the previous work of [24], a direct relation between the Yukawa coupling and the

deformation parameter is needed in order to get a localized zero mode. By setting $n = 1$, $\lambda = 0$, and $F_1 = \partial_y A(y)$ in Eq. (46), we get the zero mode solutions as

$$f_{\text{L}0,\text{R}0}(y) = \exp(\mp \eta A(y)) \tag{53}$$

that are shown in Fig. 9 for various values of p. From Fig. 9 (left), we find that the zero mode is localized on the center of the brane when $n = 1$ and $p = 1$, while it is localized between two sub-branes when $n = 1$ and $p \geq 3$. As it is seen in Fig. 9 (right), the right-handed zero mode is not localized on the brane which indicates that only one of the left- and right-handed fermion zero mode may be localized on the brane.
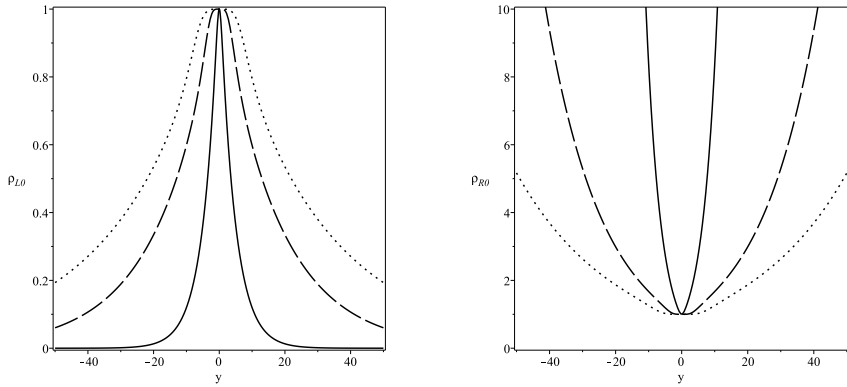

Fig. 9. The profile of (left) the left-handed zero mode and (right) the right-handed zero mode for $p = 1$ (solid line), $p = 3$ (dashed line) and $p = 5$ (dotted line). The parameters are set to $n = 1$, $\lambda = 0$ and $\eta = -1$.

Now, let us investigate the localization of the fermion zero mode under the derivative coupling mechanism. By setting $\eta = 0$ and $F_2(y) = A^m(y)$ in Eq. (46), the zero mode of fermion can be obtained as

$$f_{\text{L}0,\text{R}0}(y) = \exp(\pm \lambda A^m(y)). \tag{54}$$

In order to localize the zero modes on the deformed brane, we need to consider the following asymptotic behavior of the normalization condition which is obtained from equation (48)

$$\int_{-\infty}^{\infty} \exp\left(\frac{|y|}{p} + 2\lambda \left(-\frac{|y|}{p} \right)^m \right) \mathrm{d}y < \infty. \tag{55}$$

It is clear that the normalization condition is satisfied if

$$\begin{cases} \lambda > \frac{1}{2}, & m = 1, \\ \lambda > 0, & m = 3, 5, 7, \ldots \\ \lambda < 0, & m = 2, 4, 6, \ldots \end{cases} \tag{56}$$

The left-handed zero mode (54) is plotted in Fig. 10 for various values of p and m. As the figures show, when $m = 1$ and $p = 1$, the zero mode is localized on the single brane, while for $m \geq 2$ and $p \geq 3$, the zero mode is localized between the two sub-branes.
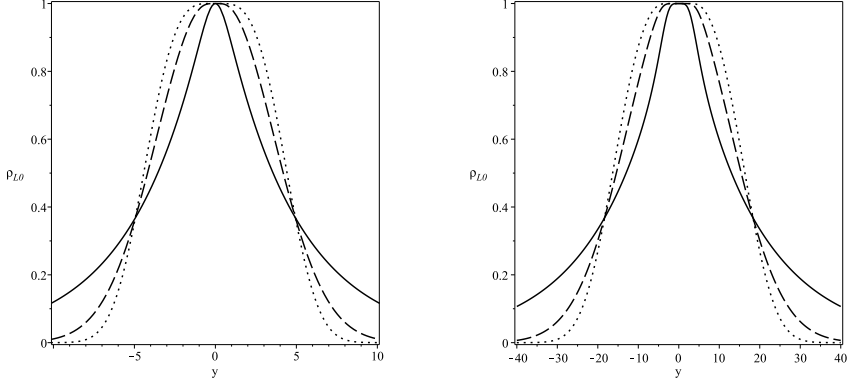

Fig. 10. The profile of the left-handed zero mode for (left) $p = 1$ and (right) $p = 3$. The parameters are set to $\eta = 0$, $\lambda = 1$ and $m = 1$ (solid line), $\lambda = -1$ and $m = 2$ (dashed line), $\lambda = 1$ and $m = 3$ (dotted line).

Finally, we investigate the normalization condition (48) for the derivative and Yukawa couplings mechanism with $\eta \neq 0$ and $\lambda \neq 0$. For simplicity, we first concentrate on the cases of $n = 1$ and $m = 1$. By considering the asymptotic behavior of the warp factor, the asymptotic behavior of the normalization condition is $\exp(-(\frac{2\gamma-1}{p})|y|) < \infty$ that is satisfied when $\gamma > \frac{1}{2}$. For $n \geq 1$ and $m \geq 1$, it can be easily found that the asymptotic behavior of the normalization condition at $y \to \pm\infty$ is

$$\begin{cases} \exp\left(2\lambda\left(-\frac{|y|}{p}\right)^m + (1+2\eta)\frac{|y|}{p}\right) < \infty, & n = 1 \quad \text{and} \quad m \geq 1, \\ \exp\left(2\lambda\left(-\frac{|y|}{p}\right)^m + \frac{|y|}{p}\right) < \infty, & n \geq 3 \quad \text{and} \quad m \geq 1. \end{cases} \tag{57}$$

Therefore, we conclude that by using the derivative and Yukawa couplings mechanism, the left-handed fermion zero mode can be localized on the deformed brane under following conditions:

$$\begin{cases} \lambda - \eta > \frac{1}{2}, & n = 1, \quad m = 1, \\ \lambda > 0, & n \geq 3, \quad m = 1, \end{cases} \tag{58}$$

and

$$\begin{cases} \lambda < 0 & n \geq 1, \quad m = 2, 4, 6, \ldots \\ \lambda > 0 & n \geq 1, \quad m = 3, 5, 7, \ldots \end{cases} \tag{59}$$

Note that for $m \geq 2$, the asymptotic behavior of the normalization condition for this case is independent of η. The profile of the left-handed zero mode is plotted for some values of m and n in Fig. 11. From these figures, we find that the zero mode is localized on the center of brane when the parameter n, m, and p simultaneously are equal to one. We note that for $p \geq 3$, $m = 1$ and $n = 1$ the zero mode is localized between the two sub-branes. We also find that for other values of n, m and p when a deformed brane splits into two sub-branes, the zero mode is localized on each sub-brane.
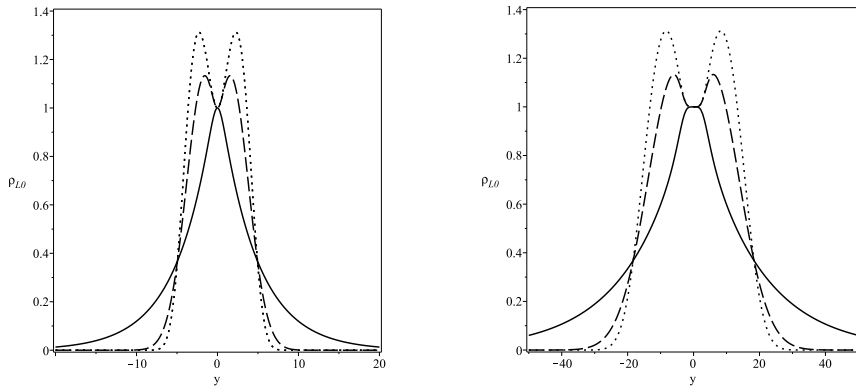

Fig. 11. The profile of the left-handed zero mode for (left) $p = 1$ and (right) $p = 3$ with $\lambda = 2$ and $m = 1$ (solid line), $\lambda = -2$, and $m = 2$ (dashed line), $\lambda = 2$ and $m = 3$ (dotted line). The parameters are set to $\eta = 1$ and $n = 1$.

5. Conclusions

In this work, by presenting the shapes of the mass-independent potentials of KK modes in the corresponding Schrödinger equations, we have investigated the localization of bulk fermion fields in a model of deformed branes. We have used two localization mechanisms one of which is the usual Yukawa coupling and the other is the derivative fermion–scalar coupling arising from the warp factor $A(y)$. First, we have considered the Yukawa coupling with $F_1(y) = \partial_y^n A(y)$, where the n must be an odd number in order to preserve the Z_2 symmetry of the effective potential. It was shown that the left-handed zero mode is localized on the deformed brane with the Yukawa coupling mechanism under the conditions of $n = 1$, and $\eta < -\frac{1}{2}$ which is independent of the deformation parameter p. Furthermore, we have found that the zero mode is localized on the center of the brane when $n = 1$ and $p = 1$, and is localized between two sub-branes when $n = 1$ and $p \geq 3$. Next, we have investigated the fermion localization with the derivative coupling mechanism

with $F_2(y) = A^m(y)$. Using this mechanism, when $m = 1$ and $p = 1$, the zero mode is localized on the single brane, while for $m \geq 2$ and $p \geq 3$, the zero mode is localized between the two sub-branes. We also have considered both the Yukawa coupling and the derivative coupling mechanisms in order to localize the fermion field on the deformed brane. We have found that the left-handed fermion zero mode can be localized under some conditions given by Eqs. (58) and (59). It was shown that when $n \geq 1$ and $m \geq 2$, this normalization condition is independent of η and p. Furthermore, in the case of both couplings, the zero mode is localized on the center of brane when the parameters n, m, and p simultaneously are equal to one, while for $p \geq 3$, $m = 1$ and $n = 1$, the zero mode is localized between the two sub-branes. We also found that for other values of n, m, and p when a deformed brane splits into two sub-branes, the zero mode is localized on each sub-brane.

In addition, it was shown that for all mentioned coupling mechanisms, the potential of KK modes in the corresponding Schrödinger equation is a volcano-like potential which means that the potential provides no mass gap to separate the fermion zero mode from KK modes. Effects of the deformation parameter p on the left-handed effective potential were discussed. It was found that under the Yukawa coupling and the derivative coupling mechanisms for odd values of n and m, increasing of the parameter p can make the brane splitting from a single-brane to two sub-branes for a single-kink background scalar field.

REFERENCES

[1] V.A. Rubakov, M.E. Shaposhnikov, *Phys. Lett. B* **125**, 139 (1983).

[2] R. Linares, H.A. Morales-Tecotl, O. Pedraza, *Phys. Rev. D* **81**, 126013 (2010).

[3] M.N. Smolyakov, I.P. Volobuev, *J. Exp. Theor. Phys.* **108**, 597 (2009).

[4] L. Randall, R. Sundrum, *Phys. Rev. Lett.* **83**, 3370 (1999).

[5] A. Kehagias, K. Tamvakis, *Phys. Lett. B* **504**, 38 (2001).

[6] H. Guo, Y.-X. Liu, Z.-H Zhao, F.-W. Chen, *Phys. Rev. D* **85**, 124033 (2012).

[7] D. Bazeia, L. Losano, *Phys. Rev. D* **73**, 025016 (2006).

[8] D. Bazeia, J. Menezes, R. Menezes, *Phys. Rev. Lett.* **91**, 241601 (2003).

[9] L. Randall, R. Sundrum, *Phys. Rev. Lett.* **83**, 4690 (1999).

[10] B. Bajc, G. Gabadadze, *Phys. Lett. B* **474**, 282 (2000).

[11] J. Liang, Y.-S. Duan, *Phys. Lett. B* **678**, 491 (2009).

[12] H. Guo, Y.-X. Liu, S.-W. Wei, C.-E. Fu, *Eur. Phys. Lett.* **97**, 60003 (2012).

[13] A. Neronov, *Phys. Rev. D* **64**, 044018 (2001).

[14] H. Christiansen, M. Cunha, *Eur. Phys. J. C* **72**, 1942 (2012).

[15] A. Kehagias, K. Tamvakis, *Phys. Lett. B* **504**, 38 (2001).

[16] C.A. Vaquera-Araujo, O. Corradini, *Eur. Phys. J. C* **75**, 48 (2015).

[17] A.E.R. Chumbes, J.M.H. da Silva, M.B. Hott, *Phys. Rev. D* **85**, 085003 (2012).

[18] A. Tofighi, M. Moazzen, *Int. J. Theor. Phys.* **50**, 1709 (2011).

[19] A. Melfo, N. Pantoja, J.D. Tempo, *Phys. Rev. D* **73**, 044033 (2006).

[20] A. Tofighi, M. Moazzen, *Int. J. Mod. Phys. A* **29**, 1450126 (2014).

[21] A.E.R. Chumbes, A.E.O. Vasquez, M.B. Hott, *Phys. Rev. D* **83**, 105010 (2011).

[22] L.B. Castro, *Phys. Rev. D* **83**, 045002 (2011).

[23] L.B. Castro, L.E. Arroyo Meza, *Eur. Phys. Lett.* **102**, 21001 (2013).

[24] W.T. Cruz, A.R. Gomes, C.A.S. Almeida, *Eur. Phys. J. C* **71**, 1790 (2011).

[25] C.A.S. Almeida, R. Casana, M.M. Ferreira, Jr., A.R. Gomes, *Phys. Rev. D* **79**, 125022 (2009).

[26] R.A.C. Correa, A. de Souza Dutra, M.B. Hott, *Class. Quantum Grav.* **28**, 155012 (2011).

[27] Q.-Y. Xie, J. Yang, L. Zhao, *Phys. Rev. D* **88**, 105014 (2013).

[28] N. Barbosa-Cendejas, D. Malagón-Morejón, R.R. Mora-Luna, *Gen. Relativ. Gravitation* **47**, 77 (2015).

[29] Y.-X. Liu, Z.-G. Xu, F.-W. Chen, S.-W. Wei, *Phys. Rev. D* **89**, 086001 (2014).

[30] H. Guo, Q.-Y. Xie, C.-E. Fu, *Phys. Rev. D* **92**, 106007 (2015).

[31] Q.-Y. Xie *et al.*, *Class. Quantum Grav.* **34**, 055007 (2017).

[32] Y.-Y. Li, Y.-P. Zhang, W.-D. Guo, Y.-X. Liu, *Phys. Rev. D* **95**, 115003 (2017).

[33] M. Moazzen, Z. Ghalenovi, *Ann. Phys.* **385**, 70 (2017).

[34] A. Tofighi, M. Moazzen, *Acta Phys. Pol. B* **45**, 1797 (2014).

[35] Y.-X. Liu, H. Guo, C.-E. Fu, H.-T. Li, *Phys. Rev. D* **84**, 044033 (2011).

[36] M. Moazzen, *Int. J. Mod. Phys. A* **32**, 1750058 (2017).

[37] R. Cartas-Fuentevilla *et al.*, *J. Cosmol. Astropart. Phys.* **05**, 026 (2016).

[38] Y.-X. Liu, L.-D. Zhang, S.-W. Wei, Y.-S. Duan, *J. High Energy Phys.* **0808**, 041 (2008).

[39] A. Tofighi, M. Moazzen, A. Farokhtabar, *Int. J. Theor. Phys.* **55**, 1105 (2016).

[40] W.T. Cruz, M.O. Tahim, C.A.S. Almeida, *Phys. Lett. B* **686**, 259 (2010).

[41] W.T. Cruz, A.R. Gomes, C.A.S. Almeida, *Eur. Phys. Lett.* **96**, 31001, (2011).

[42] W.T. Cruz, M.O. Tahim, C.A.S. Almeida, *Eur. Phys. Lett.* **88**, 41001 (2009).

[43] K. Skenderis, P.K. Townsend, *Phys. Lett. B* **468**, 46 (1999).

[44] D. Bazeia, A.R. Gomes, *J. High Energy Phys.* **0405**, 012 (2004).

[45] A. Campos, *Phys. Rev. Lett.* **88**, 141602 (2002).

[46] A. de Souza Dutra, A.C. Amaro de Faria, Jr., M. Hott, *Phys. Rev. D* **78**, 043526 (2008).

[47] C.A. Vaquera-Araujo, O. Corradini, *Eur. Phys. J. C* **75**, 48 (2015).

[48] Y.-X. Liu *et al.*, *Phys. Rev. D* **80**, 065019 (2009).

[49] D. Bazeia, A. Gomes, L. Losano, *Int. J. Mod. Phys. A* **24**, 1135 (2009).

[50] B.V. Numerov, *Mon. Not. R. Astron. Soc.* **84**, 592 (1924).

[51] B.R. Johnson, *J. Chem. Phys.* **67**, 4086 (1977).

[52] R. Landim, G. Alencar, M. Tahim, R. Costa Filho, *J. High Energy Phys.* **1108**, 071 (2011).

[53] R. Landim, G. Alencar, M. Tahim, R. Costa Filho, *J. High Energy Phys.* **1202**, 073 (2012).

[54] G. Alencar, R. Landim, M. Tahim, R. Costa Filho, *J. High Energy Phys.* **1301**, 050 (2013).